Acta Histochemica 117 (2015) 76–82

Contents lists available at ScienceDirect

Acta Histochemica

journal homepage: www.elsevier.de/acthis

Expression patterns of CD66a and CD117 in the mouse submandibular gland

Akira Takeyama [a,*], Yoshihiro Yoshikawa [b], Takashi Ikeo [b], Shosuke Morita [a], Yohki Hieda [c]

[a] Department of Oral and Maxillofacial Surgery 1, Osaka Dental University, Osaka, Japan
[b] Department of Biochemistry, Osaka Dental University, Osaka, Japan
[c] Department of Biology, Osaka Dental University, Osaka, Japan

ARTICLE INFO

Article history:
Received 17 September 2014
Received in revised form 9 November 2014
Accepted 10 November 2014

Keywords:
Salivary gland
CD66a
CD117
Stem cells
Mice

ABSTRACT

The epithelial tissue of the salivary gland consists of the acinar and ductal parts, the latter of which is further divided into the intercalated, striated and excretory duct segments and is the residential site for salivary stem/progenitor cells. In the present study, the expression patterns of two cell surface molecules, CD66a and CD117, were investigated in the adult mouse submandibular glands (SMG) by immunofluorescence microscopy. Combinations of the two molecules differentially marked several types of SMG epithelial cells, including acinar cells (CD66a-intense, CD117-negative), intercalated duct cells (CD66a-intense, CD117-positive), a subset of the striated and excretory duct cells (CD66a-weak, CD117-positive). Most of the CD117-positive ductal cells were negative for cytokeratin 5 and overlapped with the NKCC1-expressing cells. The CD117- and keratin 5-positive cells resided only in the excretory duct were suggested to correspond to the recently identified salivary stem cells. CD66a and CD117 may be useful markers to isolate several cell types consisting of SMG epithelium and to analyze their molecular and cellular nature. Our data also suggest that CD117-expressing epithelial cells of the gland include at least two distinct populations of the stem/progenitor cells.

Introduction

The salivary glands consist of acinar and ductal parts, the latter of which are further segmented into the intercalated, striated, and excretory duct regions. Saliva is secreted by acinar cells and modified during the passage through ducts to the oral cavity (Lee et al., 2012; Zhang et al., 2013). Severe decrease in saliva secretion under certain conditions, including Sjögren syndrome and radiotherapy for head and neck cancer, causes xerostomia (dry mouth) and severe dental caries and oral disorders (Burlage et al., 2001; Lee and Le, 2008; Vissink et al., 2010). No satisfactory treatment for salivary gland hypofunction is currently available. An approach that offers the possibility of restoring the damaged glands is stem cell therapy (Coppes and Stokman, 2011). In order to develop stem cell therapy, an understanding at the molecular and cellular levels of properties of undifferentiated stem/progenitor cells as well as differentiated cells of salivary glands and of mechanisms of cell differentiation is required.

Stem/progenitor cells of the salivary gland have been demonstrated to reside in the ducts. Duct ligation of the salivary gland causes atrophy with loss of acinar cells and, after the removal of the ligation the remaining ductal cells proliferate and regenerate functional acini (Takahashi et al., 1998). Cell labeling experiments also suggested the location of stem/progenitor cells in the intercalated ducts (Denny and Denny, 1999; Man et al., 2001; Kimoto et al., 2008). Direct evidence for the existence of the progenitor cell population in the ducts of the gland was obtained by lineage tracing of cells expressing Ascl3, a transcription factor specifically expressed by a subset of the ductal cells (Yoshida et al., 2001; Bullard et al., 2008). Ascl3-expressing ductal cells had the ability to differentiate into both acinar and ductal cell types; however, they had little self-renewal activity, suggesting that they are progenitor but not stem cells (Bullard et al., 2008; Arany et al., 2011; Rugel-Stahl et al., 2012).

Recently, cell surface molecules CD117 (also referred to as c-Kit) and Sca-1, which are expressed by ductal cells in salivary glands, have been used to isolate putative stem/progenitor cells from the adult mouse SMG (Hisatomi et al., 2004; Lombaert et al., 2008; Feng et al., 2009; Nanduri et al., 2013; Xiao et al., 2014). The existence of cells with stem/progenitor cell activities in the CD117-expressing population was demonstrated by the *in vitro* sphere formation and

* Corresponding author at: Department of Oral and Maxillofacial Surgery 1, Osaka Dental University, Kuzuhahanazono 8-1, Hirakata, Osaka 573-1121, Japan.
E-mail address: akiratakeyama@me.com (A. Takeyama).

http://dx.doi.org/10.1016/j.acthis.2014.11.004
0065-1281/

in vivo transplantation assays (Lombaert et al., 2008, 2013; Nanduri et al., 2013). A small fraction of cultured SMG cells proliferated to form spheres with differentiated acinar and ductal cells and, following the transplantation of CD117-expressing cells isolated from the spheres into irradiated mouse SMGs, the saliva secretion of the mice was partially restored. More recently, it was furthermore demonstrated that, of the different cells isolated from the mouse SMG, the $Lin^{-}CD24^{+}CD117^{+}Sca1^{+}$ population exhibited the highest activity for proliferation, self-renewal and differentiation *in vitro* and *in vivo* (Xiao et al., 2014). It is far less understood, however, how salivary stem/progenitor cells identified so far relate to each other.

In the present study, we analyzed in detail the expression patterns of CD117 and CD66a in the adult mouse SMG, comparing them with those of several marker molecules. CD66a, also known as CEACAM1a, a member of the Ig superfamily of cell adhesion molecules, is expressed in various epithelial tissues including developing mouse SMG (Horst et al., 2006; Leung et al., 2006; Yokoyama et al., 2007; Mima et al., 2013) and has been used to isolate living cells (Gu et al., 2010). Our present data indicate that several epithelial cell types of adult mouse SMG, including acinar and ductal cells, are differentially marked by combinations of CD117 and CD66a, and provide immunohistochemical evidence for the heterogeneity of CD117-expressing cells.

Materials and methods

Animals and tissues

Eight-week-old virgin mice (ddY strain) were purchased from Japan SLC (Hamamatsu, Shizuoka, Japan). The SMGs were dissected in Hanks' balanced salt solution (HBSS) (Sigma-Aldrich, St. Louis, MO, USA), followed by the removal of the sublingual glands and attached fat tissues. SMGs were used for preparation of tissue sections and single cells. For preparation of tissue sections, SMGs were embedded in O.C.T. compounds (Sakura Finetek Japan, Tokyo, Japan), frozen in liquid nitrogen, and kept at −80 °C until use. Frozen sections (7 μm thick) were cut. All animal experiments were performed according to the Ethical Committee on Animal Testing of Osaka Dental University.

Dissociated cell preparation

Freshly prepared SMGs were minced on ice in HBSS with fine forceps and then digested with collagenase/hyaluronidase solution (StemCell Technologies, Vancouver, Canada) in DMEM/F12 containing Glutamax (GIBCO, Carlsbad, CA, USA) supplemented with 2% heat-inactivated fetal bovine serum (FBS) at 37 °C for 1 h using a rotator (30 rpm). The digested samples were washed with HBSS supplemented with 2 mM EDTA (HE) and centrifuged at 400 rpm for 1 min, which resulted in the enrichment of epithelial organoids in the pellet. The organoids were further digested with 0.25% trypsin (Sigma-Aldrich, St. Louis, MO, USA) for 20 min at 4 °C and then with dispase (5 mg/ml; StemCell Technologies) and DNase (200 μg/ml; StemCell Technologies) for 5 min. The digested cells were centrifuged and resuspended in HE supplemented with 2% FBS (HES), and then gently passed through 23-gauge syringes followed by filtration through 40 μm cell strainers (BD Biosciences). Ten SMGs yielded $1.0–1.5 \times 10^{7}$ cells. For immunostaining, single cells were spun down onto glass slides using a Cytospin (ThermoFisher, Waltham, MA, USA) at 350 rpm and air-dried.

Immunofluorescence microscopy

Tissue sections and single cells were fixed in cold methanol for 10 min at −20 °C. In some cases, tissue sections were incubated in

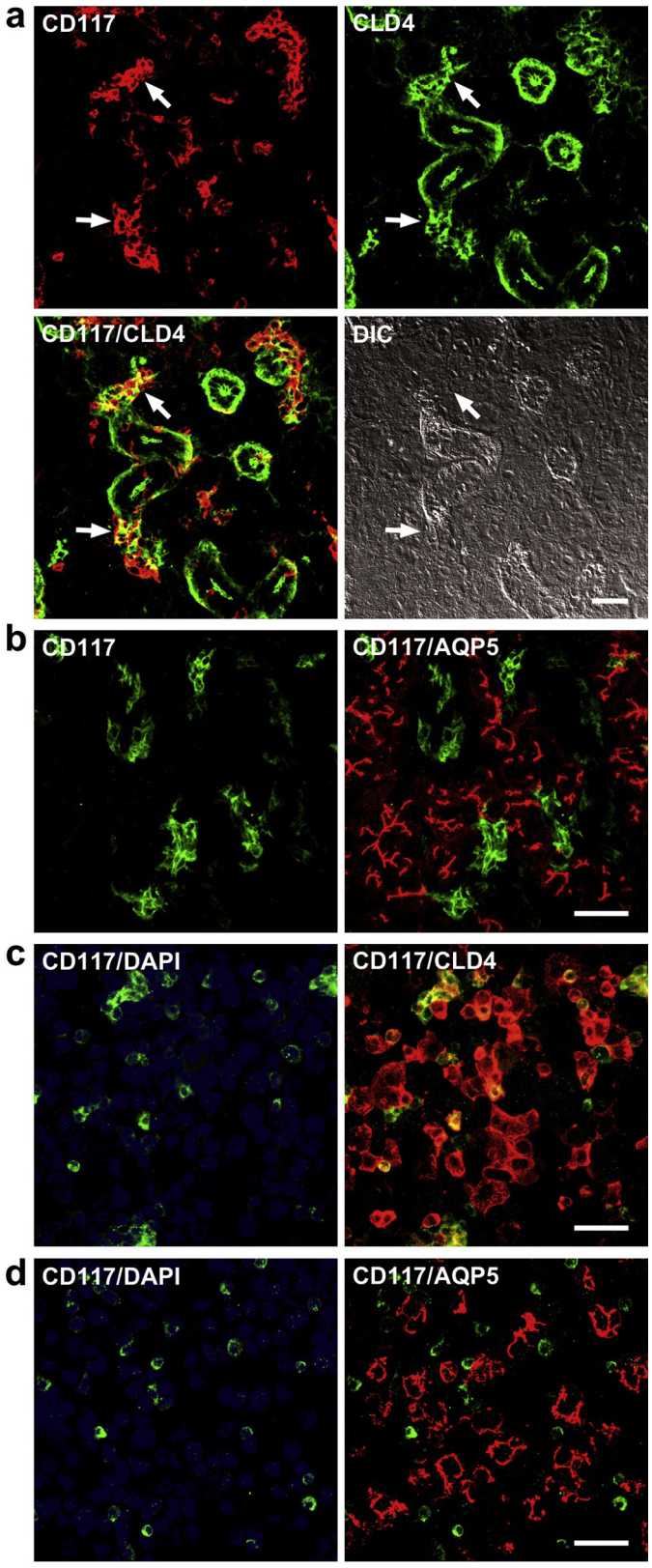

Fig. 1. (a, b) Tissue sections of the adult mouse SMG were stained for CD117 and either CLD4 or AQP5. CD117 expression is seen in CLD4-positive ducts but not AQP5-positive acini. CD117-expressing cells cluster at the CLD4-positive region (arrows) adjacent to the striated ducts and are sparsely distributed in the striated ducts. (c, d) Dissociated cells prepared from the adult mouse SMG were stained for CD117 and either CLD4 or AQP5. CD117-expressing cells are positive for CLD4 but not AQP5. Nuclei are counterstained with DAPI. DIC, differential interference contrast microscopy. Scale bars = 25 μm.

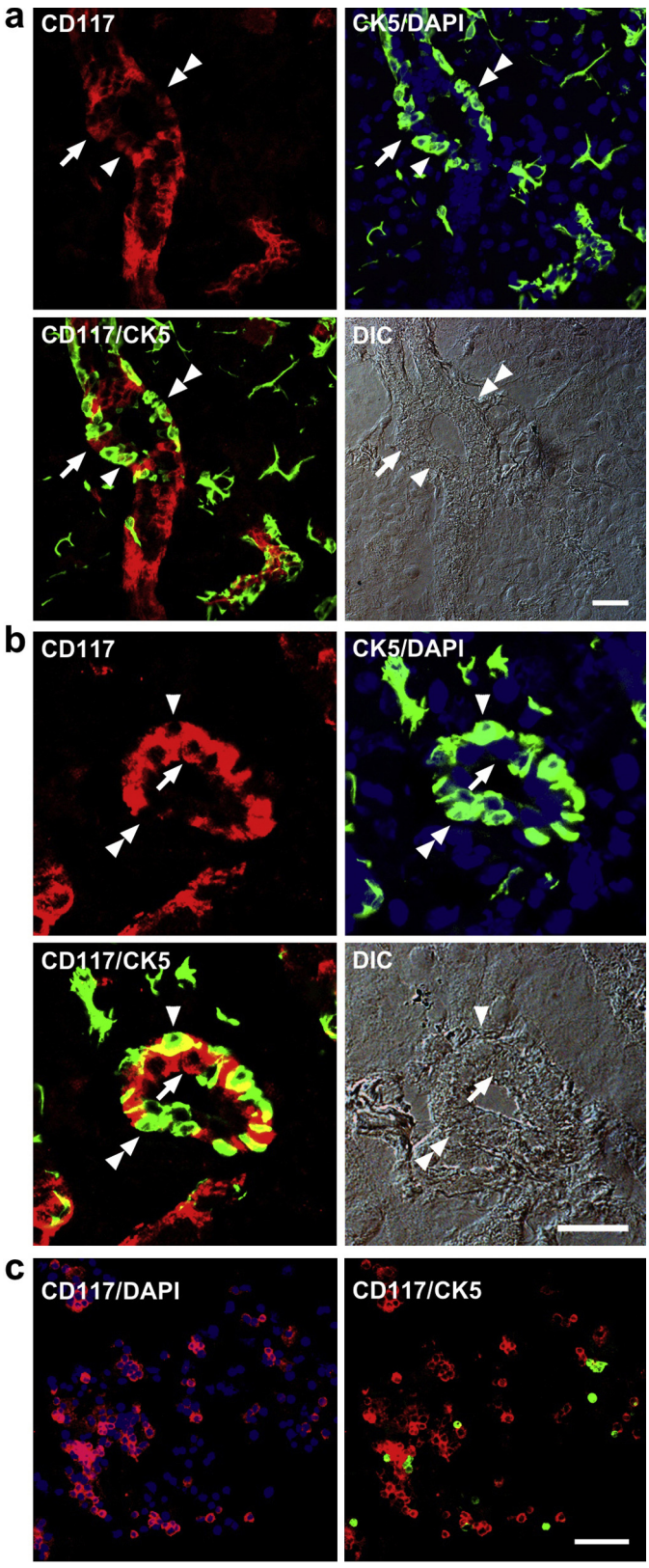

Fig. 2. (a, b) Tissue sections of the adult mouse SMG were stained for CD117 and CK5. A longitudinal view (a) and a cross section view (b) of the excretory duct are shown. Arrowheads indicate cells positive for both CD117 and CK5; arrows, cells positive for CD117 but not CK5; and double arrowheads, cells positive for CK5 but not CD117. (c) Dissociated cells prepared from the adult mouse SMG were stained for CD117 and CK5. Most of the CD117-expressing cells are negative for CK5; however, a small fraction of them are positive for CK5 (arrows). Nuclei are counterstained with DAPI. DIC, differential interference contrast microscopy. Scale bars = 25 μm (a, b), 50 μm (c).

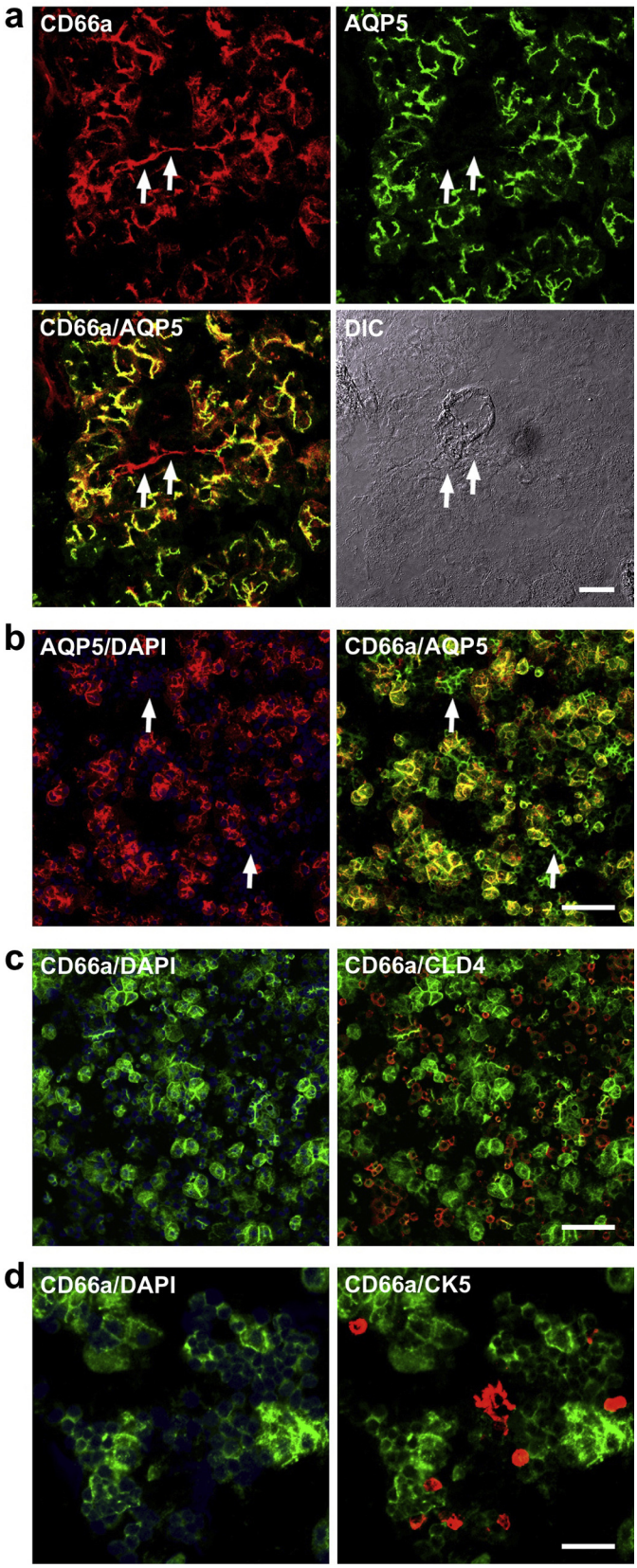

Fig. 3. (a) Tissue sections of the adult SMG were stained for CD66a and AQP5. The intense CD66a staining is seen in AQP5-positive acini, extending to the AQP5-negative region (arrows) adjacent to the striated duct. (b–d) Dissociated cells were stained for CD66a and either AQP5, CLD4 or CK5. Most of the CD66a-intense cells are positive for AQP5, and most of the CD66a-weak cells are positive for CLD4 and CK5. Note some of the CD66a-intense cells are AQP5-negative and CLD4-positive. DIC, differential interference contrast microscopy. Scale bars = 25 μm.

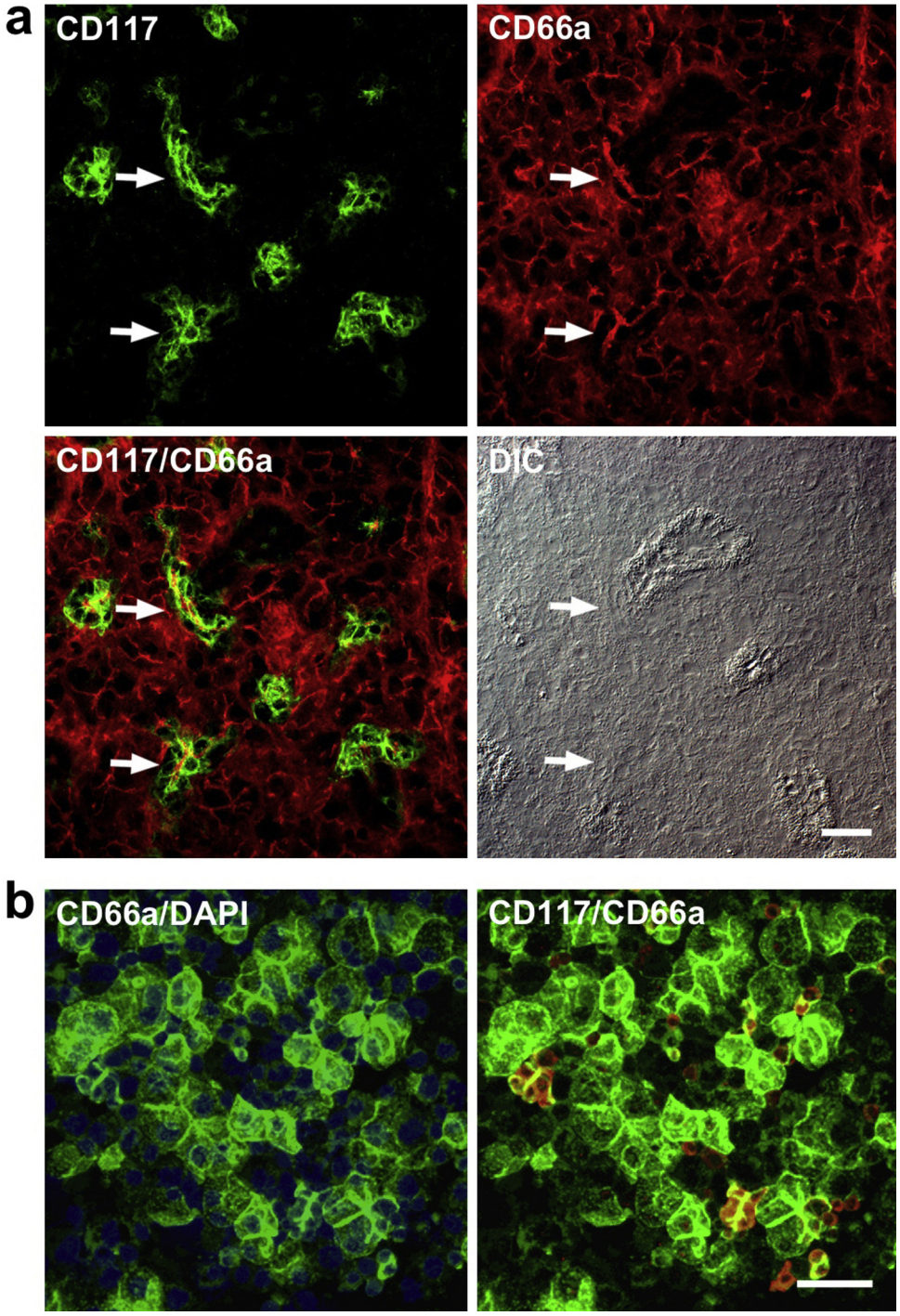

Fig. 4. Tissue sections (a) and dissociated cells (b) of the adult mouse SMG were stained for CD117 and CD66a. Clusters of CD117-expressing cells (arrows) in the vicinity of the striated duct are intensely stained for CD66a. DIC, differential interference contrast microscopy. Scale bars = 25 μm.

0.1% Triton X-100 in phosphate buffered saline (PBS) for 10 min at room temperature. After washing in PBS and incubation with 1% bovine serum albumin (BSA) in PBS for 10 min, specimens were incubated with primary antibodies diluted in 1% BSA/PBS for 1 h at room temperature or overnight at 4 °C, and then with fluorescein-conjugated secondary antibodies diluted in 1% BSA/PBS for 1 h at room temperature. After washing in PBS, specimens were mounted in ProLong Gold antifade reagent with DAPI (GIBCO) and observed with an Olympus BX-50 and Zeiss LSM700 microscope. Images were processed with ImageJ (NIH) and Photoshop (Adobe, San Jose, CA, USA).

Antibodies

Primary antibodies used were biotinylated mouse anti-CD66a (clone CC1) (BioLegend, San Diego, CA, USA), goat anti-CD117 (R&D, Minneapolis, MN, USA), rat anti-CD117 (clone ACK2) (BioLegend), goat anti-E-cadherin (R&D), mouse anti-E-cadherin (clone 36) (Transduction Laboratories, San Jose, CA, USA), rabbit anti-aquaporin 5 (Calbiochem, San Diego, CA, USA), rabbit anti-claudin 4 (provided by M. Furuse), rabbit anti-NKCC1 (provided by J. Turner), and rabbit anti-cytokeratin 5 (BioLegend). Secondary antibodies used were all donkey antibodies labeled with Alexa Fluor488 and

Alexa Fluor555 (GIBCO). For detection of biotinylated anti-CD66a, Alexa Fluor488-labeled streptavidin (GIBCO) was used.

Results and discussion

Expression patterns of two cell surface molecules CD117 and CD66a were examined in the adult mouse SMG. Immunostaining of tissue sections showed that both molecules were expressed mainly in the epithelial tissue marked by E-cadherin (data not shown). Two different antibodies against CD117 gave similar staining patterns (data not shown). As the staining intensity for the two molecules varied within the tissue, their expression patterns were analyzed in detail with tissue sections and dissociated cells, comparing with the expression of several marker molecules.

CD117 expression in the SMG was compared with the acinar marker of the water channel aquaporin-5 (AQP5) (Delporte and Steinfeld, 2006) and the ductal marker of the tight junction protein claudin-4 (CLD4) (Hashizume et al., 2004; Peppi and Ghabriel, 2004). In tissue sections, CD117 expression was detectable in CLD4-positive ducts, but not in AQP5-positive acini (Fig. 1a and b), as previously reported (Lombaert et al., 2008, 2013; Nanduri et al., 2013). Close inspection in combination with DIC (differential interference contrast) observation demonstrated that CD117-expressing cells were distributed sparsely in the striated and excretory ducts and also clustered at the CLD4-positive region in the vicinity of the striated ducts (Fig. 1a). The CLD4 positivity, AQP5 negativity and the unique location of the clustering CD117-exprssing cells suggested that they resided in the intercalated duct region, confirming the recent report by Lombaert et al. (2013). The number of CD117-expressing cells appeared larger in the excretory duct than the striated duct. Confirming the tissue section observations, analysis with dissociated cells prepared from the SMG epithelium-rich fraction showed that CD117 was detectable in some of the CLD4-positive cells (Fig. 1c) but not in the AQP5-positive cells (Fig. 1d).

CD117 expression was then compared with that of cytokeratin 5 (CK5), which is expressed by the basal cells of the excretory ducts and myoepithelial cells surrounding the acini and intercalated ducts. Although the expression of CD117 and CK5 are involved with stem/progenitor cells of salivary glands (Lombaert et al., 2008; Feng et al., 2009; Knox et al., 2010; Lombaert and Hoffman, 2010; Xiao et al., 2014), comparative analyses of their expression patterns in the adult glands have not been reported. In the excretory duct, four types of cells regarding the expression of CD117 and CK5 were recognized, including cells positive for both CD117 and CK5, positive either for CD117 or for CK5, and negative for both molecules (Fig. 2a and b). These cells were frequently noticed to associate with each other. CK5-positive cells also surrounded the CD117-expressing cell clustering in the intercalated duct region; however, co-localization of CD117 and CK5 was not recognizable (Fig. 2a). Together with the finding that the CD117-expressing cell clusters were positive for the tight junction protein CLD4 (Fig. 1a), it is suggested that these cells are the luminal cells of intercalated ducts, but not myoepithelial cells. CK5-positive cells were undetectable in the striated duct. Consistent with the tissue section observations, only a small fraction of CD117-expressing cells was positive for CK5 (Fig. 2c).

In contrast to CD117, CD66a was expressed in the entire epithelium, with the staining intensity different between acini and ducts. CD66a staining in tissue sections was intense in acini, overlapping with AQP5 staining at the luminal cell surfaces, and was faint in the striated and excretory ducts. Notably, the intense CD66a staining extended from the AQP5-positive acini to the AQP5-negative region adjacent to the striated ducts (Fig. 3a). Analysis with dissociated cells also showed the existence of two populations of

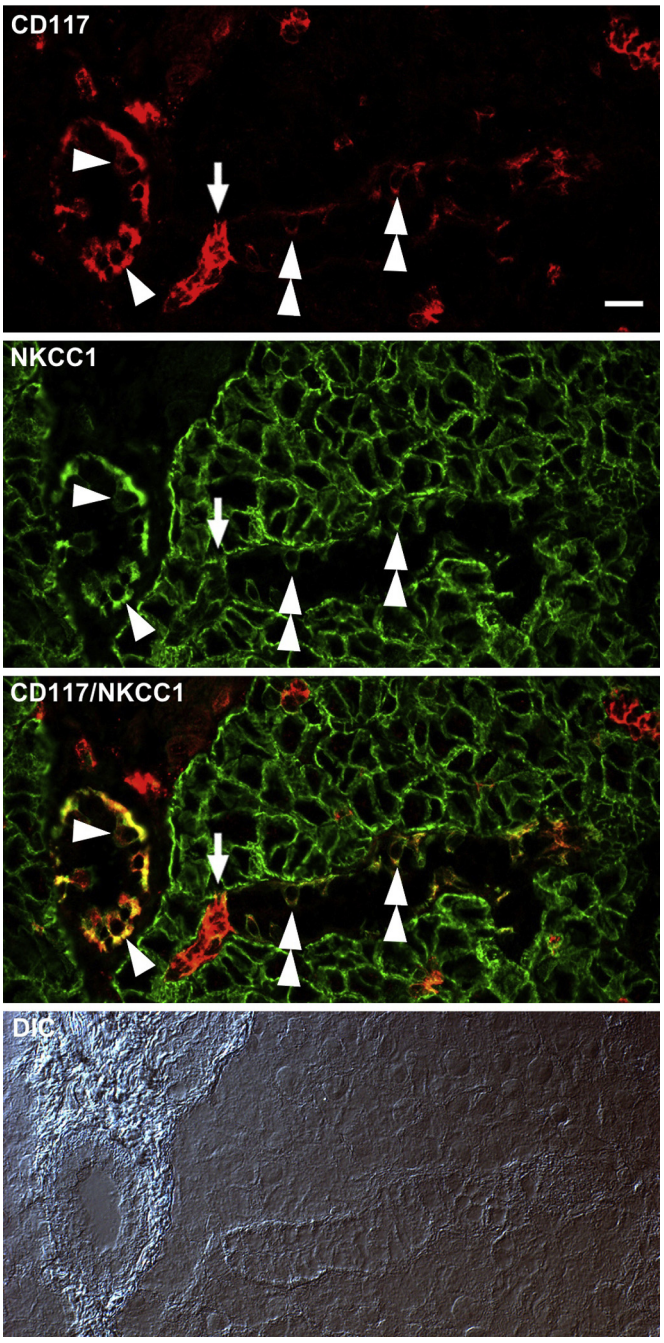

Fig. 5. Tissue sections of the adult mouse SMG were stained for CD117 and NKCC1. CD117-expresing cells in the striated (double arrowheads) and excretory (arrowheads) ducts co-localize with NKCC1. Also, CD117-expressing intercalated duct cells are positive for NKCC1 (arrow). DIC, differential interference contrast microscopy. Scale bar = 25 μm.

CD66a-positive cells, that is, CD66a-intense and -weak populations. All of the AQP5-positive cells were CD66a-intense (Fig. 3b), most of the CLD4-positive cells were CD66a-weak while the rest of them were CD66a-intense (Fig. 3c), and all of the CK5-positive cells were CD66a-weak (Fig. 3d).

As expected from the above data, the CD117-positive, intercalated duct cells were intensely stained with CD66a (Fig. 4a). Analysis with dissociated cells also showed that some of the CD117-positive cells were intensely stained for CD66a (Fig. 4b). The above findings together indicate that several cell types consisting of the SMG epithelial tissue are distinguished by combinations of two cell

surface molecules CD117 and CD66a, including acinar cells that are CD117-negative and CD66a-intense, intercalated duct cells that are CD117-positive and CD66a-intense, some of the striated and excretory duct cells that are CD117-positive and CD66a-weak, and the rest of the ductal cells and myoepithelial cells that are CD117-negative and CD66a-weak.

Like CD117-expressing cells, Ascl3-expressing progenitor cells of the SMG were previously shown to reside sparsely in the striated and excretory ducts, co-localizing with cells expressing NKCC1, a sodium–potassium–chloride co-transporter (He et al., 1997; Arany et al., 2011). As revealed by double staining of tissue sections, CD117 staining indeed overlapped with NKCC1 staining in the ductal parts (Fig. 5). As far as examined, cells of the ductal parts were either positive or negative for both CD117 and NKCC1. In addition, the CD117-expressing intercalated duct cells clustering near the striated ducts were positive for NKCC1. Thus, it is suggested that the Ascl3-expressing progenitor cells is a subpopulation of the CD117-expressing cells. As many CD117-expressing cells were negative for CK5 (Fig. 2), the CD117-positive, CK5-negative population may include the Ascl3-expressing progenitor cells.

Recently, it was demonstrated that, of the CD117-expressing cells isolated from the adult mouse SMG, $Lin^{-}CD24^{+}CD117^{+}Sca1^{+}$ population exhibited the highest activity for proliferation, self-renewal and differentiation *in vitro* and *in vivo* (Xiao et al., 2014). The residential site of $Lin^{-}CD24^{+}CD117^{+}Sca1^{+}$ stem cells in the SMG is not clear; however, the stem cell population was reported to include CK5-expressing cells and our data showed that a small fraction of the CD117-expressing cells resident in the excretory duct were positive for CK5. Thus, some of the $Lin^{-}CD24^{+}CD117^{+}Sca1^{+}$ stem cells likely reside in the excretory duct. Our data confirm the notion that there exist multiple types of stem/progenitor cells in the CD117-expressing population of the adult mouse SMG (Lombaert et al., 2013; Nanduri et al., 2013).

In conclusion, our present study shows that several types of SMG-constituting cells are discriminated by differential expression of CD117 and CD66a, confirming the heterogeneous nature of the CD117-expressing progenitor cells resident in the ducts. The use of the two cell surface markers may be useful to isolate and analyze the molecular and cellular nature of the CD117-expressing progenitor cells.

Acknowledgements

We would like thank Dr. Furuse and Dr. Turner for antibodies and Dr. Fujita and Dr. Kajimura for encouragement. We thank the Institute of Dental Research at Osaka Dental University for cell preparation and imaging facility. AT was supported by Terayama Foundation, BioLegend/Tomy Digital Biology Research Grant Program 2012/2013, and Osaka Dental University Research Funds. YH was supported by the Grant-in-Aid for Scientific Research No. 23659864 from JSPS.

References

Arany S, Catalán MA, Roztocil E, Ovitt CE. Ascl3 knockout and cell ablation models reveal complexity of salivary gland maintenance and regeneration. Dev Biol 2011;353:180–93.

Bullard T, Koec L, Roztocil E, Kingsley PD, Mirels L, Ovitt CE. Ascl3 expression marks a progenitor population of both acinar and ductal cells in mouse salivary glands. Dev Biol 2008;320:72–8.

Burlage FR, Coppes RP, Meertens H, Stokman MA, Vissink A. Parotid and submandibular/sublingual flow during high dose radiotherapy. Radiother Oncol 2001;61:271–4.

Coppes RP, Stokman MA. Stem cells and the repair of radiation-induced salivary gland damage. Oral Dis 2011;17:143–53.

Delporte C, Steinfeld S. Distribution and roles of aquaporins in salivary glands. Biochim Biophys Acta 2006;1758:1061–70.

Denny PC, Denny PA. Dynamics of parenchymal cell division, differentiation, and apoptosis in the young adult female mouse submandibular gland. Anat Rec 1999;254:408–17.

Feng J, van der Zwaag M, Stokman MA, van Os R, Coppes RP. Isolation and characterization of human salivary gland cells for stem transplantation to reduce radiation-induced hyposalivation. Radiother Oncol 2009;92:466–71.

Gu A, Zhang Z, Zhang N, Tsark W, Shively JE. Generation of human CEACAM1 transgenic mice and binding of *Neisseria* Opa protein to their neutrophils. PLoS ONE 2010;5:e10067.

Hashizume A, Ueno M, Furuse M, Tsukita S, Nakanishi Y, Hieda Y. Expression patterns of claudin family of tight junction membrane proteins in developing mouse submandibular gland. Dev Dyn 2004;231:425–31.

He X, Tse CM, Donowitz M, Alper SL, Gabriel SE, Baum BJ. Polarized distribution of key membrane transport proteins in the rat submandibular gland. Pflugers Arch 1997;433:260–8.

Hisatomi Y, Okumura K, Nakamura K, Matsumoto S, Satoh A, Nagano K, et al. Flow cytometric isolation of endodermal progenitors from mouse salivary gland differentiate into hepatic and pancreatic lineages. Hepatology 2004;39:667–75.

Horst AK, Ito WD, Dabelstein J, Schumacher U, Sander H, Turbide C, et al. Carcinoembryonic antigen-related cell adhesion molecule 1 modulates vascular remodeling in vitro and in vivo. J Clin Invest 2006;116:1596–605.

Kimoto M, Yura Y, Kishino M, Toyosawa S, Ogawa Y. Label-retaining cells in the rat submandibular gland. J Histochem Cytochem 2008;56:15–24.

Knox SM, Lombaert IM, Reed X, Vitale-Cross L, Gutkind JS, Hoffman MP. Parasympathetic innervation maintains epithelial progenitor cells during salivary organogenesis. Science 2010;329:1645–7.

Lee NY, Le QT. New developments in radiation therapy for head and neck cancer: intensity-modulated radiation therapy and hypoxia targeting. Semin Oncol 2008;35:236–50.

Lee MG, Ohara E, Park HW, Yang D, Muallem S. Molecular mechanism of pancreatic and salivary gland fluid and HCO_3 secretion. Physiol Rev 2012;92:39–74.

Leung N, Turbide C, Olson M, Marcus V, Jothy S, Beauchemin N. Deletion of the carcinoembryonic antigen-related cell adhesion molecule 1 (CEACAM1) gene contributes to colon tumor progression in a murine model of carcinogenesis. Oncogene 2006;25:5527–36.

Lombaert IMA, Brunsting JF, Wierenga PK, Faber H, Stokman MA, Kok T, et al. Rescue of salivary gland function after stem cell transplantation in irradiated glands. PLoS ONE 2008;3:e2063.

Lombaert IMA, Hoffman MP. Epithelia stem/progenitor cells in the embryonic mouse submandibular gland. Front Oral Biol 2010;14:90–100.

Lombaert IMA, Abrams SR, Li L, Eswarakumar VP, Sethi AJ, Witt RL, et al. Combined KIT and FGFR2b signaling regulates epithelial progenitor expansion during organogenesis. Stem Cell Rep 2013;1:604–19.

Man YG, Ball WD, Marchetti L, Hand AR. Contributions of intercalated duct cells to the normal parenchyma of submandibular glands of adult rats. Anat Rec 2001;263:202–14.

Mima J, Koshino A, Oka K, Uchida H, Hieda Y, Nohara M, et al. Regulation of the epithelial adhesion molecule CEACAM1 is important for palate formation. PLoS ONE 2013;8:e61653.

Nanduri LSY, Lombaert IMA, van der Zwaag M, Faber H, Brunsting JF, van Os RP, et al. Salisphere derived c-Kit+ cell transplantation

restores tissue homeostasis in irradiated salivary gland. Radiother Oncol 2013;108:458–63.
Peppi M, Ghabriel MN. Tissue-specific expression of the tight junction proteins claudins and occluding in the rat salivary glands. J Anat 2004;205:257–66.
Rugel-Stahl A, Elliot ME, Ovitt CE. Ascl3 marks adult progenitor cells of the mouse salivary gland. Stem Cell Res 2012;8:379–87.
Takahashi S, Schoch E, Walker NI. Origin of acinar cell regeneration after atrophy of the rat parotid induced by duct obstruction. Int J Exp Pathol 1998;79:293–301.
Vissink A, Mitchell JB, Baum BJ, Limesand KH, Jensen SB, Fox PC, et al. Clinical management of salivary gland hypofunction and xerostomia in head-and-neck cancer patients: success and barriers. Int J Radiat Oncol Biol Phys 2010;78:983–91.
Xiao N, Lin Y, Cao H, Sirjani D, Giaccia AJ, Koong AC, et al. Neurotrophic factor GDNF promotes survival of salivary stem cells. J Clin Invest 2014;124:3364–77.
Yokoyama S, Chen CJ, Nguyen T, Shively JE. Role of CEACAM1 isoforms in an in vitro model of mammary morphogenesis: mutational analysis of the cytoplasmic domain of CEACAM1-4s reveals key residues involved in lumen formation. Oncogene 2007;26:7637–46.
Yoshida S, Ohbo K, Takakura A, Takebayashi H, Okada T, Abe K, et al. Sgn1, a basic helix-loop-helix transcription factor delineates the salivary gland duct cells lineage in mice. Dev Biol 2001;240:517–30.
Zhang GH, Wu LL, Yu GY. Tight junctions and paracellular fluid and ion transport in salivary glands. Clin J Dent Res 2013;16:13–46.